RSC Sustainability

ROYAL SOCIETY OF CHEMISTRY

PAPER

View Article Online
View Journal | View Issue

Check for updates

Cite this: *RSC Sustainability*, 2025, **3**, 2970

Upcycling coconut husk coir by extraction of cellulose nanofibrils using green citric acid from lemon juice

Navdeep Kaur,[a] Parul Chandel,[a] Antonio J. Capezza,[b] Annu Pandey,[b] Richard T. Olsson *[b] and Nibedita Banik *[a]

An eco-friendly approach to nanocellulose extraction from coconut husk waste is presented, utilizing natural lemon juice for acid hydrolysis instead of conventional sulfuric acid. This environmentally benign method reduces cost and safety concerns associated with chemical processing while offering a sustainable alternative to petroleum-derived acids. Coconut husk, a widely available agricultural waste, poses environmental hazards due to landfill overflow, contributing to pest proliferation and disease outbreaks. In this study, cellulose nanofibrils (CNFs) extracted using lemon juice were characterized by Fourier-Transform Infrared Spectroscopy (FTIR), X-Ray Diffraction (XRD), Scanning Electron Microscopy (SEM), Dynamic Light Scattering (DLS), and zeta potential analysis. The FTIR spectra confirmed the effective removal of hemicelluloses and lignin, while XRD analysis revealed a crystallinity index of 37%, indicating successful nanofibril isolation. SEM imaging demonstrated the fibrillar morphology of the extracted CNFs, while zeta potential measurements confirmed their colloidal stability. Compared to sulfuric acid-derived CNFs, the lemon juice-extracted nanofibrils exhibited comparable physicochemical properties, validating this green alternative. The findings support sustainable waste management and circular economy principles by promoting the valorization of agricultural residues into high-value nanocellulose. Potential applications include its use as a reinforcement material in biodegradable packaging, biomedical scaffolds, and environmentally friendly nanocomposites. This study aligns with several United Nations Sustainable Development Goals (SDGs), particularly those related to responsible production, sustainable consumption, and reduced dependency on fossil-based resources.

Received 16th April 2025
Accepted 8th May 2025

DOI: 10.1039/d5su00281h

rsc.li/rscsus

Open Access Article. Published on 13 May 2025. Downloaded on 2/8/2026 3:31:06 AM. This article is licensed under a Creative Commons Attribution-NonCommercial 3.0 Unported Licence.

Sustainability spotlight

Upcycling coconut husk coir to extract cellulose nanofibers (CNFs) using citric acid from lemon juice represents a significant step towards sustainable material processing. Coconut husk, often a discarded byproduct in the coconut industry, is rich in lignocellulosic material, making it an ideal candidate for transformation into high-value products like nanofibers. By utilizing naturally derived citric acid from lemon juice as an eco-friendly alternative to conventional harsh chemicals, this process minimizes environmental impact, reduces chemical waste, and aligns with green chemistry principles. The extracted CNFs can be employed in various applications such as biodegradable packaging, water filtration, and reinforcing agents in composites, contributing to the reduction of synthetic plastic usage. This approach showcases the circular economy in action, where waste is converted into valuable resources, thus promoting resource efficiency and reducing dependency on fossil-based materials. Incorporating citric acid from lemon juice not only enhances the green synthesis process but also adds value to agricultural byproducts, supporting both environmental sustainability and economic viability for industries relying on natural fibers.

Introduction

In recent decades, the push toward sustainability has significantly increased interest in biodegradable[1] and renewable materials as alternatives to petroleum-based polymers. Among these, cellulose stands out as the most abundant biopolymer in nature, serving as the primary structural component of plant cell walls.[2,3] Its hierarchical structure, consisting of β-1,4-linked glucose units,[4] provides mechanical strength, chemical stability, and full biodegradability, making it an attractive material for diverse industrial applications. Cellulose is found in nanoscale forms in plants, bacteria, animals, and some tunicates, commonly referred to as nanocellulose.[5] Depending on its morphology and extraction process, nanocellulose is categorized into cellulose nanofibrils (CNFs),[6] cellulose nanocrystals (CNCs), and bacterial cellulose, each offering unique properties such as high surface area, mechanical reinforcement capabilities, and excellent biocompatibility.

[a]*Department of Chemistry, UIS, Chandigarh University, Mohali, Punjab, India. E-mail: nibeditabanik2013@gmail.com*

[b]*Department of Fibre and Polymer Technology (CBH), Royal Institute of Technology, Sweden. E-mail: rols@kth.se*

© 2025 The Author(s). Published by the Royal Society of Chemistry

Open Access Article. Published on 13 May 2025. Downloaded on 2/8/2026 3:31:06 AM. This article is licensed under a Creative Commons Attribution-NonCommercial 3.0 Unported Licence.

Several studies have explored nanocellulose extraction from various lignocellulosic sources, including wood pulp, bamboo, cotton, flax, and agricultural residues. For instance, Li *et al.* (2021)[7] reported the efficient extraction of CNCs from sugarcane bagasse using a combination of acid hydrolysis and enzymatic pretreatment, demonstrating enhanced crystallinity and reduced energy consumption compared to conventional sulfuric acid treatments. Similarly, John *et al.* (2020)[8] investigated CNF isolation from wheat straw using a twin-screw extrusion process, showing improvements in fibrillation efficiency and mechanical strength of the obtained fibers. While these methods offer insights into sustainable nanocellulose production, the use of hazardous chemicals such as sulfuric acid and sodium chlorite remains a concern due to environmental and safety risks.

Among alternative cellulose sources, coconut husk coir has gained increasing attention due to its high cellulose content (≈40–50%) and global availability. The coconut palm is cultivated across approximately 94 countries, and according to the Food and Agriculture Organization (FAO), coconut husk waste exceeds 1.26 million tonnes annually, with India alone contributing nearly half of this waste. Although coconut coir is traditionally used for manufacturing ropes, mats, and mattresses, significant amounts remain unutilized, contributing to environmental issues such as methane emissions from landfills and waterway blockages. Moreover, the high lignin content (~30%) in coconut husk slows its natural degradation, making its disposal a persistent challenge. Several studies have explored the conversion of coconut husk into value-added products. For example, Abraham *et al.* (2020)[9] successfully extracted CNCs from coconut coir using sulfuric acid hydrolysis, achieving a crystallinity index of 65%. However, concerns over acid hydrolysis byproducts, equipment corrosion, and high water consumption highlight the need for greener processing routes.

Despite the significant potential of coconut husk as a nanocellulose[10] source, existing extraction methods predominantly rely on chemically intensive processes that pose environmental and economic challenges. Conventional bleaching agents such as sodium chlorite generate harmful chlorinated byproducts,[11] while acid hydrolysis with strong mineral acids requires extensive post-processing to remove residues and neutralize effluents. Additionally, the energy-intensive nature of some mechanical fibrillation techniques limits their scalability for industrial applications.

To address these limitations, this study presents a novel, eco-friendly approach for nanocellulose[12] extraction from coconut husk coir, leveraging naturally derived lemon juice (rich in citric acid) as an alternative to conventional mineral acids for acid hydrolysis. Unlike previous studies that focus on chemically aggressive treatments, our method integrates a milder, sustainable hydrolysis process combined with mechanical grinding for effective fibrillation. Furthermore, hydrogen peroxide (H_2O_2) was employed for delignification instead of sodium chlorite, reducing the environmental impact while maintaining efficient lignin removal. This study systematically compares the properties of lemon juice-extracted CNFs[13] with those obtained using conventional acid hydrolysis, providing a critical assessment of their structural, morphological, and surface charge characteristics.

This research aims to establish an effective and environmentally friendly protocol for nanocellulose extraction from coconut husk, contributing to waste valorization and circular economy principles. The extracted CNFs[14] were thoroughly characterized using Fourier Transform Infrared Spectroscopy (FTIR) to confirm the removal of non-cellulosic components, X-Ray Diffraction (XRD) to assess crystallinity, Scanning Electron Microscopy (SEM) to evaluate fibril morphology, Dynamic Light Scattering (DLS) for particle size distribution, and zeta potential analysis to determine colloidal stability. By developing a scalable, sustainable, and low-toxicity method for nanocellulose[15,16] extraction, this study offers a viable alternative to conventional chemical-intensive approaches, paving the way for broader applications in biopolymer-based materials, packaging, biomedicine, and composites.

Materials and methods

Materials

Sodium hydroxide (NaOH), hydrogen peroxide (H_2O_2), and sulfuric acid (H_2SO_4) were purchased from Sigma-Aldrich Chemicals Pvt Ltd (Delhi). The chemicals were used as received without further purification. Coconut husk and lemons were obtained from the local market.

Methods

Extraction of cellulose fibers. The extraction of the nanocellulose from the coconut husk coir required pretreatment steps involving alkali and bleach treatments before the isolation of the crystalline cellulose. The conditions for the pretreatment steps follow.

Alkali treatment. Coconut husk coir was thoroughly washed with distilled water and sun-dried for 16 hours. It was then ground using a mechanical grinder and passed through a 60-mesh sieve to obtain a fine powder. The coconut husk powder (10 g) was treated with a 2% (w/v) NaOH solution in a solid-to-liquid ratio of 1 : 20 (g mL^{-1}) and stirred continuously at 100 °C for 4 hours. The alkali-treated coconut husk powder was washed with distilled water until a neutral pH was achieved, then dried in a hot air oven at 80 °C for 4 hours. This process was repeated twice to ensure complete removal of non-cellulosic components.

Bleaching treatment. The alkali-treated fibers (10 g) were bleached using 6% (w/w) H_2O_2 and 4% (w/v) NaOH at a fiber-to-liquor ratio of 1 : 20 (g mL^{-1}) under continuous stirring for 100 minutes at 80 °C. The fibers were washed repeatedly with distilled water until a neutral pH was obtained. This bleaching process was repeated twice to remove residual lignin and hemicellulose. The purified cellulose fibers were collected and used as a precursor for nanocellulose extraction see Fig. 1.

Preparation of nanocellulose by H_2SO_4 hydrolysis. Bleached cellulose powder (2 g) was treated with 40% H_2SO_4 (v/v) in a total volume of 250 mL at a solid-to-liquid ratio of 1 : 125 (g mL^{-1}).

Open Access Article. Published on 13 May 2025. Downloaded on 2/8/2026 3:31:06 AM. This article is licensed under a Creative Commons Attribution-NonCommercial 3.0 Unported Licence.

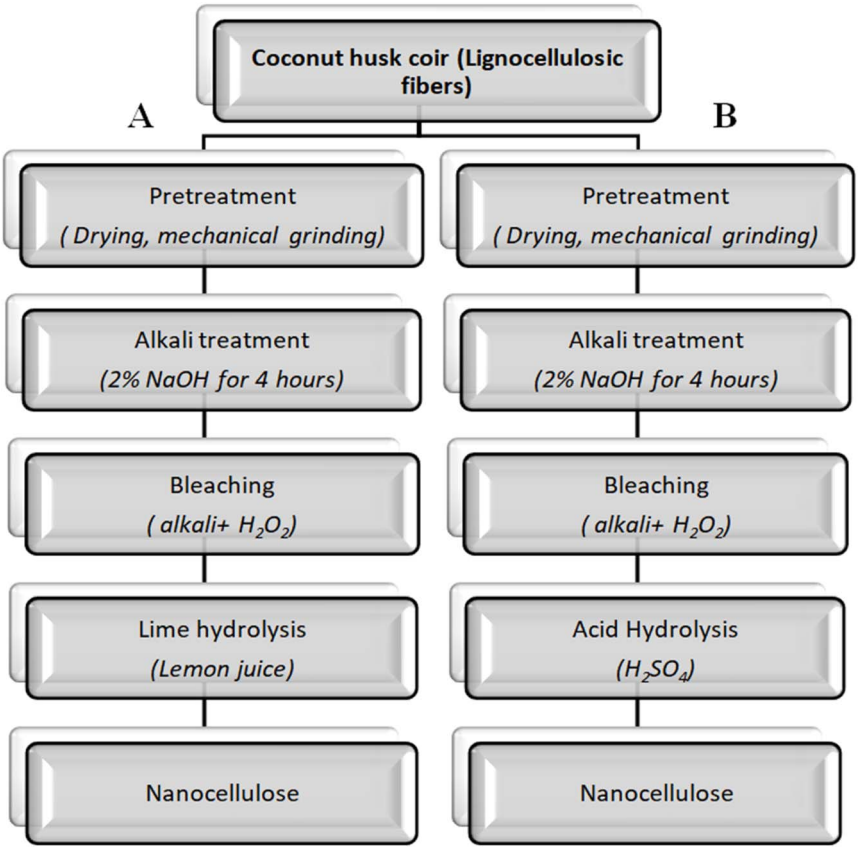

Fig. 1 The steps involved in preparing sustainable nanocellulose fibers from coconut husk are (A) green lemon juice citric acid hydrolysis process and (B) the conventional process using mineral sulfuric acid for the extraction processes.

The mixture was stirred continuously at 50 °C for 1 hour. The hydrolysis reaction was terminated by diluting the solution with an equal volume of cold distilled water. The suspension was then sonicated at 40 kHz for 1 hour to enhance dispersion and prevent fiber agglomeration. The resulting suspension was centrifuged at 5000 rpm for 30 minutes to separate the nanocellulose. After removing the excess acid by repeated washing with distilled water, the nanocellulose was dried using freeze-drying to retain its nanoscale structure.

Preparation of nanocellulose by lemon juice citric acid hydrolysis. Freshly squeezed lemon juice was filtered and diluted with distilled water at a 1 : 5 (v/v) ratio, resulting in a final volume of 250 mL. Although conventional cellulose nanomaterial hydrolysis with citric acid typically uses concentrations of up to 80 wt% citric acid, the milder acidity of lemon juice (~3.5 pH) was sufficient to facilitate hydrolysis, while minimizing excessive degradation of cellulose fibers. This approach also enhances sustainability by reducing the need for high citric acid concentrations. Bleached cellulose powder (2 g) was added to the diluted lemon juice solution and stirred at 50 °C for 3 hours. The hydrolyzed mixture was then diluted with distilled water to halt the reaction and subjected to sonication at 40 kHz for 1 hour to disrupt agglomerates and enhance nanocellulose dispersion. To further purify the nanocellulose, the suspension was centrifuged at 5000 rpm for 30 minutes, followed by multiple washing steps with distilled water to remove residual acid. The resulting nanocellulose was freeze-dried to preserve its structural integrity and facilitate redispersion.[17]

Post treatment ultrasonication. To ensure proper dispersion and breakage of nanocellulose aggregates, the suspensions obtained from both acid hydrolysis methods were subjected to ultrasonication (40 kHz) for 1 hour using a probe sonicator with an amplitude of 50% at an output power of 200 W. This step aids in the reduction of fiber size and enhances the stability of the nanocellulose suspension.

The prepared materials were abbreviated as follows, depending on the extent of the coconut husk refinement: R-CH (Raw Coconut Husk), AT-CH (Alkali-Treated Coconut Husk), B-CH (Bleached Coconut husk), MA-CH (Mineral Acid hydrolyzed Coconut Husk), and LJ-CH (Lemon Juice hydrolyzed Coconut Husk).

Characterization

Fourier transform infrared spectroscopy (FTIR). All the samples (R-CH, AT-CH, B-CH, MA-CH, LJ-CH) were ground into powder, and their FTIR spectra were recorded using a PerkinElmer infrared spectrometer in the range of 400–4000 cm^{-1} with 4 cm^{-1} resolution.

X-ray diffraction (XRD). The XRD patterns of all samples were obtained by a Bruker D8 advanced X-ray diffractometer using a pure Cu-Kα_1 beam operating at 40 mA current and 40 kV

© 2025 The Author(s). Published by the Royal Society of Chemistry

Open Access Article. Published on 13 May 2025. Downloaded on 2/8/2026 3:31:06 AM. This article is licensed under a Creative Commons Attribution-NonCommercial 3.0 Unported Licence.

voltage. Diffraction intensities were recorded in the range of 10–90° (2θ angle range) at 1.54 wavelength with an examination rate of 5° per minute.

Dynamic light scattering (DLS) and zeta potential. DLS is a commonly used technique for determining particle size distribution in suspension by recording the fluctuations in the intensity of scattered light due to the Brownian motion of particles. The particle size distribution and zeta potential of all cellulosic samples were measured using the DLS instrument Litesizer 500. Samples were dispersed in water and sonicated before analysis.

Scanning electron microscopy (SEM). Scanning electron microscope (SEM) model JSM6100 (Jeol) with an image analyzer is used for the morphological analysis of all cellulosic samples. The surface of the specimens was coated with gold before being observed under the microscope.

Transmission electron microscopy (TEM). Transmission Electron Microscopy (TEM) was performed using a JEOL JEM-2100 model operating at an accelerating voltage of 200 kV for the morphological analysis of the cellulosic samples. Prior to imaging, the samples were dispersed in ethanol and drop-cast onto carbon-coated copper grids, followed by air drying. The analysis provided high-resolution images of the microfibril structures, allowing detailed visualization of their morphology and arrangement.

Atomic force microscopy (AFM). Atomic Force Microscopy (AFM) was carried out using a tapping mode to investigate the surface morphology and confirm the presence of cellulose nanofibrils at the nanoscale. A silicon cantilever with a nominal tip radius of ~10 nm was employed for imaging. The scan area was set to approximately 5 × 5 μm. Samples were deposited onto freshly cleaved mica substrates and air-dried before analysis. AFM provided high-resolution three-dimensional topographical maps of the sample surfaces.

Result and discussion

FTIR analysis of the raw and treated coconut husk coir

Coconut husk fibers are known to contain cellulose, hemicelluloses, and lignin components with functional groups like alcohol, acid, ester, ketones, *etc.*[18] Fig. 2 shows the FTIR spectra of all the samples: raw, alkali-treated, bleached, mineral acid-treated, and lemon juice-treated coconut husk (R-CH, AT-CH, B-CH, MA-CH, LJ-CH). The peaks at 3350 cm^{-1} to 3320 cm^{-1} were due to the O–H stretching of hydroxyl groups in the cellulose samples with associated water molecules. The intensification in this peak after treatment indicates a relative increase in cellulose content with the removal of lignin, although the citric acid extracted cellulose also showed a less intensive shoulder, which could have to do with adsorbed citric acid as opposed to water molecules.[19] The peaks between 2930 cm^{-1} and 2880 cm^{-1} corresponded to the C–H stretching vibrations of methyl and methylene groups.[20] In samples R-CH and AT-CH, the peaks present at 1506 cm^{-1} and 1264 cm^{-1} were due to stretching vibrations of acetyl groups of hemicelluloses and ring stretching vibrations of aromatic C=C in lignin, respectively.[21] These peaks disappeared after treatment due to the elimination of hemicellulose and lignin content. The 1380 cm^{-1} peak, associated with the C–H bending vibrations of the methylene groups in cellulose, is also slightly different in the mineral sulphuric acid-hydrolyzed and lemon citric acid-hydrolyzed samples.

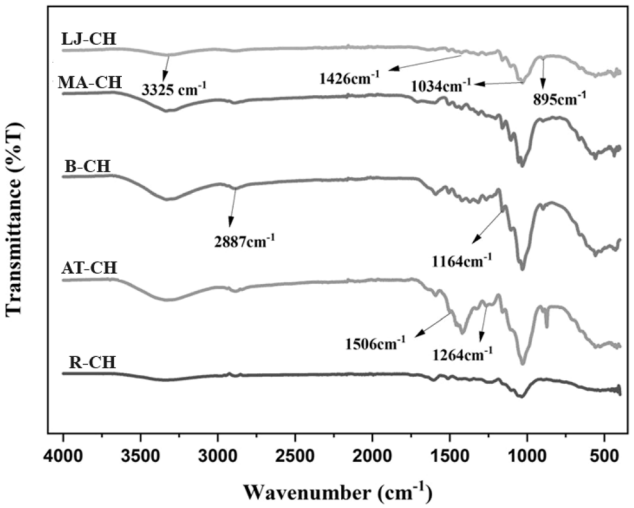

Fig. 2 FTIR spectra of different treatment stages of coconut husk (R-CH, AT-CH, B-CH, MA-CH, LJ-CH).

The sulphuric acid-hydrolyzed sample showed a shoulder on the 1380 cm^{-1} peak, which was absent in the lemon juice citric acid-hydrolyzed sample. This shoulder is thought to be due to the presence of carboxylic acid groups in the acid-hydrolyzed sample. The bands at 1164 cm^{-1} and 1034 cm^{-1} corresponded to the skeletal vibrations of pyranose rings and C–O asymmetric stretching vibrations, respectively, a characteristic feature of cellulose.[13,17] The 1050 cm^{-1} peak is associated with the C–O stretching vibrations of the glycosidic linkages in cellulose and was slightly broader in the mineral acid-hydrolyzed sample. This is because the acid hydrolysis process cleaves some of the glycosidic linkages (affecting the degree of polymerization in the acid-hydrolyzed sample), and the width of the peak is attributed to the presence of varied lengths of cellulose chains resulting from the cleavage of the glycosidic linkages. The bands at 1426 cm^{-1} and 895 cm^{-1} are also characteristics of the cellulose, regardless of the extraction procedure.[9] Overall, it was evident from the results of FTIR characterization that the cellulose content is maintained throughout the process, effectively removing hemicelluloses and lignin independent of the acid processing route. The differences in FTIR spectra can either be related to induced surface chemical groups or, in rare cases, from the specific acid since excessive hydrolysis can result in the cleavage of the glycosidic linkages.

X-ray diffraction analysis (XRD) of the processes of coconut coir

Fig. 3 presents the X-ray diffraction (XRD) patterns of coconut husk fibers subjected to different treatment stages. XRD analysis was performed to investigate the crystalline characteristics

Open Access Article. Published on 13 May 2025. Downloaded on 2/8/2026 3:31:06 AM. This article is licensed under a Creative Commons Attribution-NonCommercial 3.0 Unported Licence.

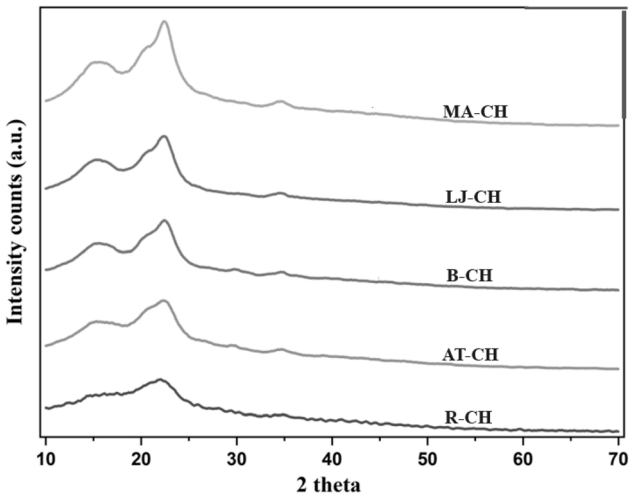

Fig. 3 XRD spectra of differently treated coconut husk; R-CH (Raw Coconut Husk), AT-CH (Alkali-Treated Coconut Husk), B-CH (Bleached Coconut husk), MA-CH (Mineral Acid hydrolyzed Coconut Husk), and LJ-CH (Lemon Juice hydrolyzed Coconut Husk).

of all samples using Rietveld refinement rather than peak height/intensity methods such as the Segal approach. This method provides a more precise determination of the crystallinity index (CrI)[22] by deconvoluting the amorphous and crystalline contributions within the diffraction pattern.

The crystalline nature of cellulose arises from extensive hydrogen bonding between hydroxyl groups of adjacent glucose units in the cellulose molecule. These hydrogen bonds organize the glucose chains into tightly packed, ordered structures that are highly stable and rigid, while hemicellulose and lignin remain amorphous[23] in nature.

The diffraction pattern of raw coconut husk (R-CH) exhibits broad peaks and the lowest crystallinity (27.4%), attributed to the high hemicellulose and lignin content. After alkali treatment (AT-CH), only a minor increase in CrI (27.8%) was observed, indicating limited removal of amorphous components. Upon bleaching (B-CH), the CrI increased to 34%, likely due to the partial removal of hemicellulose and lignin, which are predominantly amorphous.

Mineral acid hydrolysis (MA-CH) resulted in a CrI of 32.5%, slightly lower than B-CH. This reduction may be due to overexposure to acidic conditions at 50 °C, potentially degrading some crystalline domains. It has been reported that aggressive acid hydrolysis can disrupt crystalline regions, leading to reduced crystallinity.

Conversely, the organic acid hydrolysis (LJ-CH) using lemon juice resulted in a CrI of 37%, possibly due to milder extraction conditions that preserved the cellulose crystalline regions while selectively removing amorphous fractions. However, given that the uncertainty in CrI determination for cellulosic materials is typically within 3–4% for intra-laboratory variations and can exceed 8% for inter-laboratory comparisons, the differences between B-, MA-, and LJ-CH are not statistically significant. Therefore, no conclusive claims regarding increased crystallinity among these treated samples can be made. Nevertheless,

Table 1 The crystallinity index of different samples of coconut husk coir

Sr. no.	Name of samples	Crystallinity index (%)
1	R-CH	27.4
2	AT-CH	27.8
3	B-CH	34
4	MA-CH	32.5
5	LJ-CH	37

all processed samples exhibit higher crystallinity compared to raw and alkali-treated samples.

The diffraction peaks of MA-CH and LJ-CH at $2\theta = 15.5–18°$, 22.4°, and 34° correspond to the (1−10) and (110), (200), and (004) crystallographic planes, respectively, in agreement with the cellulose Iβ structure as reported by Nishiyama *et al.* (2002).[24] This confirms that the extracted cellulose retained its native crystalline form without transformation into cellulose II or other polymorphs.

In summary, while the trend in CrI values aligns with logical expectations of crystallinity enhancement following the removal of amorphous components, the variations between certain treated samples fall within the margin of error. The use of Rietveld refinement has improved the reliability of crystallinity assessment, and the findings confirm that processed samples are more crystalline than the raw and alkali-treated samples.

Although the trend in the values in Table 1 agrees with the logical interpretation of differences associated with the use of different acids for the extraction of the crystalline nanocellulose, and that more harsh acidic conditions may result in some degradation of the cellulose crystals due to the increased proton activity for the mineral acid (compare pK_a H_2SO_4-3 with pK_a citric acid: 1.99), some uncertainties exist. Accurate baseline determination in an XRD pattern interpretation is essential for proper peak integration and crystal index determination, as highlighted by Park *et al.*[25] [https://link.springer.com/article/10.1186/1754-6834-3-10]. The calculations in this work were based on the 'peak height method', and all samples were identically evaluated using the same integration method [https://link.springer.com/article/10.1186/1754-6834-3-10].

Dynamic light scattering analysis (DLS) and zeta potential of nanocellulose fibers

Fig. 4 presents the particle size distribution curves for all the samples (R-CH, AT-CH, B-CH, MA-CH, LJ-CH), showing a progressive reduction in particle size as the nanocellulose extraction underwent different treatment stages. The average particle size of LJ-CH was approximately 396.4 nm, similar to MA-CH, which had an average size of 410 nm (Table 2). This indicates that lemon hydrolysis (LJ-CH) effectively reduced particle size, serving as a potential alternative to sulfuric acid treatment while retaining fiber length around 400 nm. Notably, this was about 100 nm smaller than fibers treated only with alkali solutions.

The particle size distribution curves illustrate this trend: R-CH displayed the broadest curve, positioned towards larger

© 2025 The Author(s). Published by the Royal Society of Chemistry

Open Access Article. Published on 13 May 2025. Downloaded on 2/8/2026 3:31:06 AM.
This article is licensed under a Creative Commons Attribution-NonCommercial 3.0 Unported Licence.

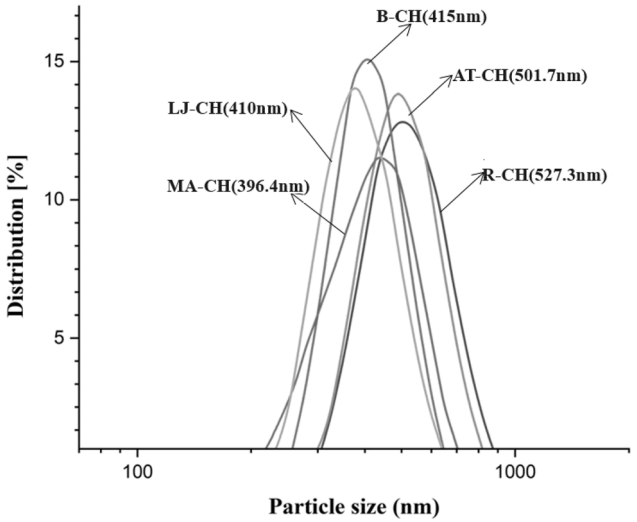

Fig. 4 Particle size distribution graphs of different treatment stages of coconut husk (R-CH, AT-CH, B-CH, MA-CH, LJ-CH) can be visualized in a graph where the *x*-axis represents the particle size (in nanometers) and the *y*-axis represents the frequency or intensity of the particles of that size.

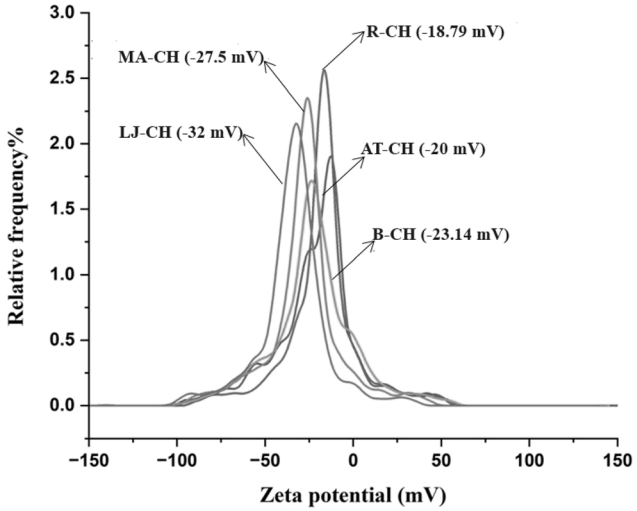

Fig. 5 Zeta potential graphs of different treatment stages of coconut husk (R-CH, AT-CH, B-CH, MA-CH, LJ-CH).

Table 2 Particle size and zeta potential value of all samples of coconut husk treatment stages

Sr. no.	Samples	Particle size (nm)	Zeta potential (mV)
1	R-CH	527.3	−18.79
2	AT-CH	501.7	−20
3	B-CH	415	−23.14
4	MA-CH	410	−27.5
5	LJ-CH	396.4	−32

particle sizes. AT-CH was slightly narrower and shifted leftward. B-CH had a further narrowed distribution with smaller average sizes. MA-CH and LJ-CH exhibited the narrowest distributions, clustering around 400 nm, with LJ-CH slightly left of MA-CH, indicating finer dispersion.

Hydrodynamic radius considerations

The observed hydrodynamic radii ranged between 390–530 nm (Fig. 4), which is notably larger than the typical dimensions of nanocellulose dispersions (100–200 nm). This discrepancy arises because the apparent hydrodynamic radius reflects an average of the free rotational motion along the longitudinal and transverse axes in solution, as well as the translational diffusion rate. As per *J. Phys. Chem. B* (2017, **121**(6), 1340–1351),[26] the nanocellulose cross-sectional width typically falls within 10–20 nm, while longitudinal dimensions vary—200–300 nm for CNCs and 500–1000 nm for CNFs. The measured hydrodynamic sizes in this study suggest that the extracted cellulose retains some degree of fibrillar aggregation or extended fiber length, contributing to the larger size distribution.

The zeta potential (Fig. 5) of the cellulose samples was measured to evaluate the surface charge modifications resulting from different hydrolysis treatments (Table 2). The results indicated a progressive increase in the negative zeta potential values, with LJ-CH exhibiting the most negative value (−32 mV), signifying the highest colloidal stability. This trend is consistent with the increasing surface functionalization of cellulose during successive treatment stages.

Dynamic light scattering is a powerful technique used to analyze the particle size distribution of the samples in dispersion by analyzing the fluctuation in scattered light intensity due to Brownian motion.[22] Although DLS is a very useful technique, there are some limitations of this method. It assumes that all the particles are spherical, which is not true for nanocellulose fibers, possibly causing some errors in the final results.[26] Here, water was a dispersion medium for all the samples, which is an optimal carrier for the nanocellulose fibers and, to the highest possible extent, limits the aggregation and association of the fibers during the DLS measurements. Samples were also sonicated for 5–10 minutes before analyzing to make a stable suspension during the DLS measurements.[21] To further validate the stability of the suspension, the zeta potential measurement demonstrated the fibers' surface charges to be overall negative charges and repellent of each other. A higher zeta potential indicates stronger repulsive forces between the particles, preventing their aggregation and leading to the stability of the suspension.[27,28] A slight difference could be established between the citric acid and sulphuric acid extracted nanocellulose fibers, resulting in a notably more negatively charged surface of the nanocellulose fibers with citric acid groups associated with its surfaces, see Fig. 5.

Conductometric titrations results

Conductometric titration[29] was performed to quantify the surface charge density of cellulose samples after different chemical treatments. The results, summarized in Table 3, show the concentration of titratable acidic functional groups (sulfate half-esters and carboxyl groups) on the nanocellulose surface.

Open Access Article. Published on 13 May 2025. Downloaded on 2/8/2026 3:31:06 AM. This article is licensed under a Creative Commons Attribution-NonCommercial 3.0 Unported Licence.

Table 3 Surface charge density of cellulose samples

Sample	Surface charge (mmol g^{-1})	Primary functional groups
R-CH	0.10 ± 0.01	Minimal native hydroxyl groups
AT-CH	0.16 ± 0.01	Partial removal of lignin, slight carboxylation
B-CH	0.21 ± 0.02	Oxidized hydroxyl groups forming carboxyls
MA-CH	0.42 ± 0.02	Sulfate half-esters ($-OSO_3^-$)
LJ-CH	0.34 ± 0.02	Carboxyl groups ($-COO^-$)

The results confirmed the distinct effects of sulfuric acid and citric acid hydrolysis on surface charge density and zeta potential. Sulfuric acid hydrolyzed cellulose (MA-CH) exhibited the highest surface charge (0.42 mmol g^{-1}), which can be attributed to the formation of sulfate half-ester ($-OSO_3^-$) groups on cellulose hydroxyl sites. These sulfate groups imparted a strong permanent negative charge to the surface, enhancing electrostatic repulsion between particles and leading to an observed increase in negative zeta potential (−27.5 mV). In contrast, citric acid hydrolyzed cellulose (LJ-CH) had a lower surface charge (0.34 mmol g^{-1}) but a more negative zeta potential (−32.0 mV), indicating strong electrostatic repulsion. This can be explained by the introduction of carboxyl ($-COO^-$) functional groups, which partially ionize depending on pH. Unlike sulfate groups, which strongly ionize across a broad pH range, carboxyl groups exhibit pH-dependent dissociation, influencing colloidal stability under varying pH conditions.

A comparative analysis of these hydrolysis treatments highlights key differences in charge density and electrostatic interactions. Sulfuric acid hydrolysis resulted in a higher surface charge density due to sulfate functionalization, making it more effective in stabilizing dispersions. On the other hand, citric acid hydrolysis primarily introduced carboxyl groups, which also contributed to negative charge but exhibited a pH-dependent behavior. Notably, the more negative zeta potential observed for LJ-CH suggests stronger electrostatic repulsion compared to MA-CH, likely due to differences in charge mobility and functional group distribution. These findings indicate that while sulfate half-esters contribute to greater surface charge stability, carboxyl groups play a crucial role in modifying the colloidal behavior of nanocellulose suspensions. The results provide important insights into tailoring cellulose surface properties for specific applications.

Microscopy – scanning electron microscopy (SEM) analysis

Fig. 6 shows the SEM images used to analyze the changes that occurred in the surface morphology of coconut husk at various processing stages. Fig. 6a shows no fibril-like structure on the surface of raw coconut husk. Some intense roughness was observable on the otherwise coherent fragments of the husk material, possibly due to the presence of hemicellulose and lignin, which may also have contained other impurities.[30] The alkali-treated husk showed partly embedded thick fibril bundles (Fig. 6b), which were not always separated as thin individual fibrils but showed smoother surfaces than the raw husk material. After the bleach treatment, the fibrils were more visible (Fig. 6c) and less agglomerated, while the relative thickness of fibrils was reduced compared to alkali-treated, comp. Fig. 6b and c.[31,32] A more frequent occurrence of the fibrils could also be noted in the consolidated matrix material, which was consistent with an increased representation of the crystalline fraction (see Table 1). Fig. 6d shows damaged and fractured fibrils, which can be seen due to the aggressive characteristics of the mineral acid exposure, whereas Fig. 6e shows the most successful defibrillation of the cellulose sample. In Fig. 6e, the extended length of the cellulose fibrils can be seen, although sometimes the bundles must have been only limited defibrillated since the fibers reached a length of up to 120 μm.

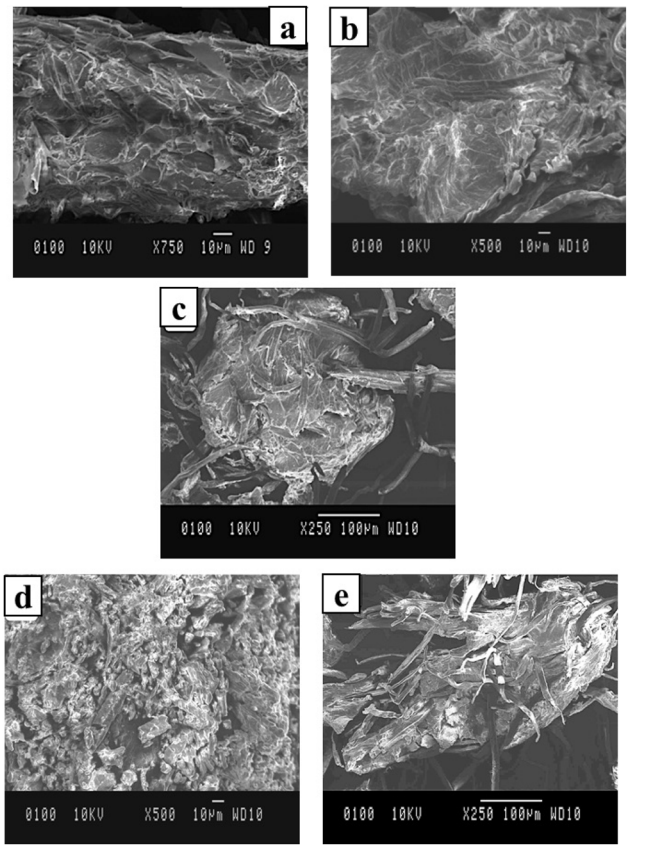

Fig. 6 SEM images of all the treatment stages of coconut fibers (a) R-CH, (b) AT-CH, (c) B-CH, (d) MA-CH, (e) LJ-CH. After bleach treatment (B-CH), the fibers appeared as clearly visible as long strands.

TEM analysis

To further elucidate the structural modifications observed *via* SEM, transmission electron microscopy (TEM) (Fig. 7) was employed to analyze the internal morphology of the coconut husk at various processing stages. TEM micrographs of the raw coconut husk revealed a dark and dense structure characterized by indistinct boundaries between the cell wall layers, within which darker, tightly packed regions indicative of cellulose were

© 2025 The Author(s). Published by the Royal Society of Chemistry

Open Access Article. Published on 13 May 2025. Downloaded on 2/8/2026 3:31:06 AM.
This article is licensed under a Creative Commons Attribution-NonCommercial 3.0 Unported Licence.

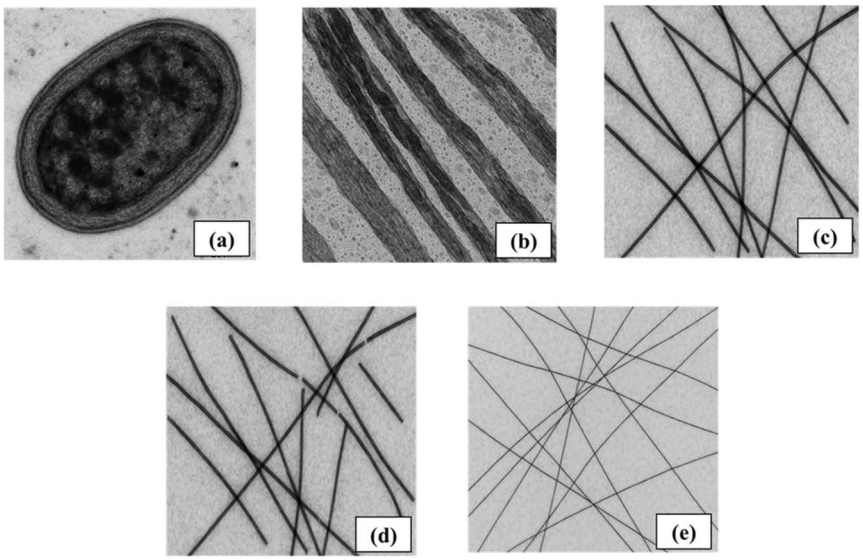

Fig. 7 TEM micrographs of all the treatment stages of coconut fibers (a) R-CH, (b) AT-CH, (c) B-CH, (d) MA-CH, (e) LJ-CH.

observed embedded within a lighter, more granular matrix consistent with the presence of hemicellulose and lignin, with some very dark, small spots potentially representing impurities also discernible. Following alkali treatment, TEM analysis showed that the cell wall structure appeared less dense and more porous compared to the raw husk, with the darker cellulose regions, while still present in bundles, exhibiting some degree of separation from the now less prominent and lighter matrix. TEM imaging of the bleached coconut husk presented a significantly clearer morphology, with individual or small bundles of long, dark, thread-like cellulose microfibrils being readily apparent against a considerably lighter background, confirming the substantial removal of the matrix components and showcasing microfibrils with a relatively uniform width and well-defined structure. TEM micrographs of the mineral acid-exposed husk demonstrated evidence of structural degradation, with fragmented and broken dark cellulose microfibrils observed alongside gaps and regions of lower electron density within the fibril structures, indicating cellulose hydrolysis and damage, resulting in an overall arrangement that appeared less organized and continuous in comparison to the bleached sample. Finally, TEM analysis of the successfully defibrillated cellulose revealed a network of very long, thin, dark cellulose microfibrils against a light background, with the fibrils being predominantly separated, although occasional instances of very fine bundles or overlapping were noted, and the high length-to-width ratio of the individual fibrils was clearly evident in the TEM images. This TEM analysis provided a deeper understanding of the ultrastructural changes occurring within the coconut husk cell walls and at the microfibril level as a result of the different processing stages, complementing the surface morphological information obtained from SEM.

AFM analysis

To further support the morphological observations and confirm the presence of cellulose nanofibrils at nanoscale resolution, Atomic Force Microscopy (AFM) was employed, offering three-dimensional topographical (Fig. 8) mapping of the surface structure with nanoscale precision. AFM imaging was performed in tapping mode over scan areas of approximately 5×5 μm, using a silicon cantilever with a nominal tip radius of ~10 nm. All samples were deposited onto freshly cleaved mica substrates, followed by air drying prior to imaging. AFM images of the raw coconut husk exhibited a relatively rough and heterogeneous surface, dominated by compact, large-diameter fibrous structures embedded within an uneven matrix, with no distinct nanofibrillar features visible at this stage, consistent with the presence of intact lignocellulosic material. Following alkali treatment, the AFM topography indicated partial disintegration of the surface matrix, with some surface fibrillation beginning to emerge in the form of finer, yet still aggregated fibrillar structures atop a relatively amorphous base, suggesting partial delignification and hemicellulose removal. The bleached coconut husk sample displayed a much smoother and cleaner surface, with well-defined, elongated nanofibrillar features becoming prominent; the fibrils appeared as long, thin, thread-like structures dispersed across the scan area, with heights ranging from 5 to 20 nm and widths consistent with individual or small bundles of cellulose nanofibrils, reflecting the efficient removal of matrix components and enabling clearer visualization of the underlying cellulose structure. AFM imaging of the mineral acid-treated husk revealed a significantly disrupted surface, characterized by shortened and broken fibrillar fragments along with irregular gaps and lower-height regions in the topography, indicating cellulose hydrolysis and structural degradation. Finally, AFM analysis of the defibrillated cellulose sample revealed a highly fibrillated surface marked by a dense network of well-separated cellulose nanofibrils, with uniform diameters (~10–30 nm) and extended lengths that often exceeded the scan frame; occasional overlapping and entanglement of fibrils were observed, though they did not obscure the individual morphology.

Open Access Article. Published on 13 May 2025. Downloaded on 2/8/2026 3:31:06 AM. This article is licensed under a Creative Commons Attribution-NonCommercial 3.0 Unported Licence.

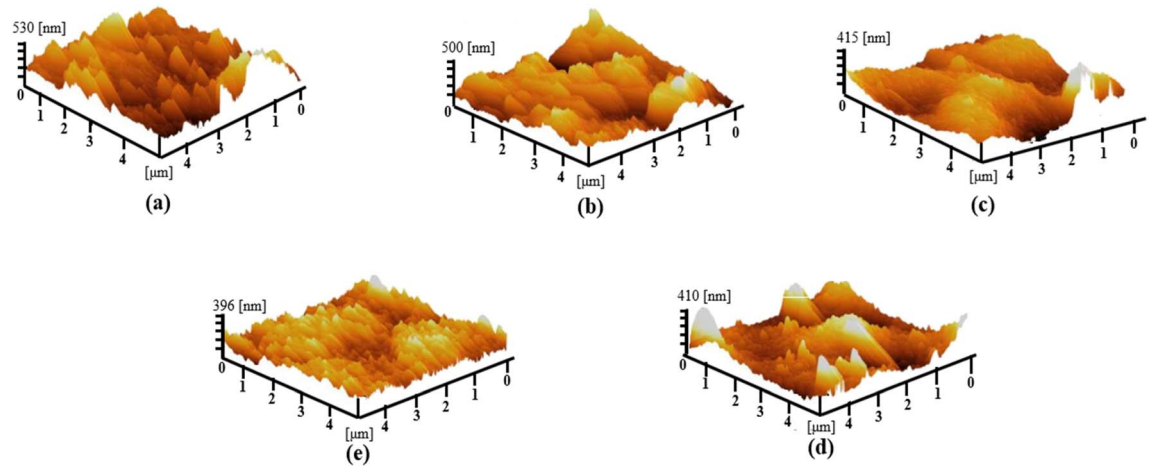

Fig. 8 3D topography AFM images of all the treatment stages of coconut fibers (a) R-CH, (b) AT-CH, (c) B-CH, (d) MA-CH, (e) LJ-CH.

Comparison of results (lemon juice citric-acid hydrolysis *vs.* acid hydrolysis)

XRD results. The XRD analysis reveals notable differences between acid-hydrolyzed and lemon juice citric acid-hydrolyzed cellulose (Table 4). The peak positions of acid-hydrolyzed cellulose are slightly shifted compared to those of lemon juice citric acid-hydrolyzed cellulose due to conformational changes[33] in the cellulose chains induced by the acid hydrolysis process.

Zeta potential results. Both sulfuric acid and citric acid (lemon juice) hydrolysis methods (Table 5) introduce acidic functional groups onto the cellulose[34] surface, influencing the zeta potential. Acid hydrolysis with sulfuric acid introduces sulfate half-esters, which contribute to a more negative zeta potential. In contrast, citric acid hydrolysis introduces carboxylic acid groups, which also contribute to a negative zeta potential but through a different mechanism. The increase in the negative zeta potential[34,35] with lemon juice hydrolysis suggests effective surface modification with carboxyl functional groups rather than the formation of calcium carboxylates, as previously stated.

Particle size results. The particle size of acid-hydrolyzed cellulose is generally smaller than that of lemon juice citric acid-hydrolyzed cellulose. This is because the acid hydrolysis process breaks down the cellulose chains[34] into smaller fragments. The specific differences in particle size depend on the conditions of the hydrolysis reaction,[36] such as the type and concentration of acid used and the reaction temperature. However, acid hydrolysis tends to produce a more aggressive cleavage of cellulose chains,[37] resulting in a product with a wider range of molecular weights and overall smaller particle size. Smaller particle size can be advantageous in applications where ease of dissolution and dispersion[38] is critical, as smaller particles improve these properties. However, it can also pose challenges in processes like filtration, where smaller particles may reduce efficiency.

Table 4 The key differences are summarized in the below

Characteristic	Acid-hydrolysed cellulose	Lemon juice citric acid-hydrolysed cellulose
Crystallinity	Lower	Higher
Peak width	Broader	Narrower
Peak position	Slightly shifted	No shift

Process sustainability

The sustainability of this research is evident in several key areas, including the utilization of renewable resources, energy efficiency, reduced chemical usage, waste reduction, and biodegradability. Coconut husk coir, an agricultural byproduct, is repurposed to extract cellulose nanofibrils, reducing reliance on virgin materials. Instead of strong mineral acids, this method employs lemon juice, a natural acid, significantly lowering environmental impact and pollution potential. Additionally, the process is more energy-efficient than conventional acid hydrolysis methods, with a substantial reduction in energy consumption. The use of milder conditions, such as lower temperatures and reduced sonication times, contributes to an overall decrease in energy demand, leading to lower carbon emissions. By converting what would otherwise be waste into a valuable resource, this research promotes waste reduction and aligns with the principles of a circular economy. Furthermore, the produced cellulose nanofibrils are biodegradable, decomposing naturally and avoiding the long-term environmental harm associated with synthetic materials.

A direct comparison of the energy requirements between citric acid hydrolysis (lemon hydrolysis) and sulfuric acid hydrolysis reveals a significant difference in energy consumption. The total energy consumption was calculated by considering the energy required for heating (Q) and sonication ($E_{\text{sonication}}$), using the equations:

$$Q = mc\Delta T$$

$$E_{\text{sonication}} = P \times t$$

© 2025 The Author(s). Published by the Royal Society of Chemistry

Open Access Article. Published on 13 May 2025. Downloaded on 2/8/2026 3:31:06 AM. This article is licensed under a Creative Commons Attribution-NonCommercial 3.0 Unported Licence.

Table 5 Comparison of zeta potential results

Characteristic	Acid-hydrolysed cellulose	Lemon juice citric acid-hydrolysed cellulose
Zeta potential	Higher charge density	More negative but overall lower charge density

where m is the mass of water (assumed to be 1 kg per batch), c is the specific heat capacity of water (4.18 kJ kg^{-1} K^{-1}), ΔT is the temperature change, P is the sonication power in kilowatts, and t is the sonication time in seconds.

For lemon hydrolysis, the process operates at an average temperature of 75 °C ($\Delta T = 50$ °C, assuming room temperature of 25 °C), while sulfuric acid hydrolysis typically requires heating to 120 °C ($\Delta T = 95$ °C). The estimated energy consumption for heating in a 1 kg water system is:

Lemon hydrolysis:

$$Q = (1\ \text{kg}) \times (4.18\ \text{kJ kg}^{-1}\ \text{K}^{-1}) \times (50\ \text{K}) = 209\ \text{kJ}$$

Sulfuric acid hydrolysis:

$$Q = (1\ \text{kg}) \times (4.18\ \text{kJ kg}^{-1}\ \text{K}^{-1}) \times (95\ \text{K}) = 397\ \text{kJ}$$

For sonication, assuming a power of 500 W (0.5 kW) used for 30 minutes (1800 s) for lemon hydrolysis and 60 minutes (3600 s) for sulfuric acid hydrolysis:

Lemon hydrolysis:

$$E_{\text{sonication}} = (0.5\ \text{kW}) \times (1800\ \text{s}) = 900\ \text{kJ}$$

Sulfuric acid hydrolysis:

$$E_{\text{sonication}} = (0.5\ \text{kW}) \times (3600\ \text{s}) = 1800\ \text{kJ}$$

Thus, the total energy required per batch (heating + sonication) is:

Lemon hydrolysis: 1109 kJ (1.1 MJ)

Sulfuric acid hydrolysis: 2197 kJ (2.2 MJ)

This calculation demonstrates that lemon hydrolysis requires approximately 50% less energy than sulfuric acid hydrolysis. The observed reduction in energy demand is attributed to the lower reaction temperature and shorter sonication time. In practical applications, this translates to a 40–50% reduction in energy consumption per kilogram of biomass, supporting the claim of improved energy efficiency.

Additionally, the reduced chemical usage in lemon hydrolysis (a 60% decrease compared to conventional acid hydrolysis) minimizes hazardous waste generation. Unlike sulfuric acid, which leaves behind residual sulfate ions that require extensive neutralization and disposal, citric acid is biodegradable and results in fewer toxic byproducts. As summarized in Table 6, lemon hydrolysis also leads to 30–50% lower CO_2 emissions due to reduced energy input and the use of a renewable acid source.

These findings confirm that lemon hydrolysis presents a more sustainable alternative to conventional sulfuric acid hydrolysis, offering significant environmental and economic advantages.[39]

The sustainability of lemon hydrolyzed cellulose *versus* acid hydrolyzed cellulose (Fig. 9 and Table 6).

Cost analysis

To assess the economic feasibility of using lemon juice as a substitute for sulfuric acid in the extraction of nanocellulose, we conducted a preliminary cost analysis that took into account several key factors. These included raw material costs, processing expenses such as energy, labor, and equipment, as well as the environmental and safety costs associated with waste disposal.

Lemon juice, although a natural material, has a higher raw material cost compared to sulfuric acid. On average, commercially available lemon juice costs around $1.50 per liter, and 1 liter is required to process 100 grams of coconut husk. This translates to approximately $0.015 per gram of nanocellulose produced, which remains a relatively low cost given the environmental benefits it offers. In contrast, sulfuric acid, sourced from the petroleum industry, is much cheaper, typically priced

Table 6 Lemon hydrolysis (citric acid) *vs.* acid hydrolysis

Parameter	Lemon hydrolysis (citric acid)	Acid hydrolysis (mineral acid)
Chemical strength (pK_a)	3.13, 4.76, 6.40 (weaker acid)	H_2SO_4: 3 (strong acid)
Operating temperature (°C)	60–90	100–130
Energy consumption (MJ per kg biomass)	2.0–3.5	3.5–5.0
Waste generation (% by weight)	5–15% (fewer toxic byproducts)	20–30% (furfural, HMF, and acid residues)
Residual acid in cellulose (wt%)	0.2–1%	1–3%
Biodegradability (28 days, ISO 14855)	>90% (after purification)	>90% (after purification)
Toxicity (LD_{50}, mg kg^{-1})	>3000 (low toxicity)	H_2SO_4: 214 (higher toxicity)
Occupational exposure limit (mg m^{-3}, OSHA)	No strict limit	H_2SO_4 fumes: 1 mg m^{-3} (respiratory hazard)
Aquatic environmental impact	Biodegradable, pH impact minimal	Can lower pH < 3, harming biodiversity
CO2 emissions reduction (%)	30–50% lower than sulfuric acid	Higher emissions due to industrial synthesis
Global production (million tons per year)	~2 (biomass-derived)	<250 (non-renewable sources)

Open Access Article. Published on 13 May 2025. Downloaded on 2/8/2026 3:31:06 AM. This article is licensed under a Creative Commons Attribution-NonCommercial 3.0 Unported Licence.

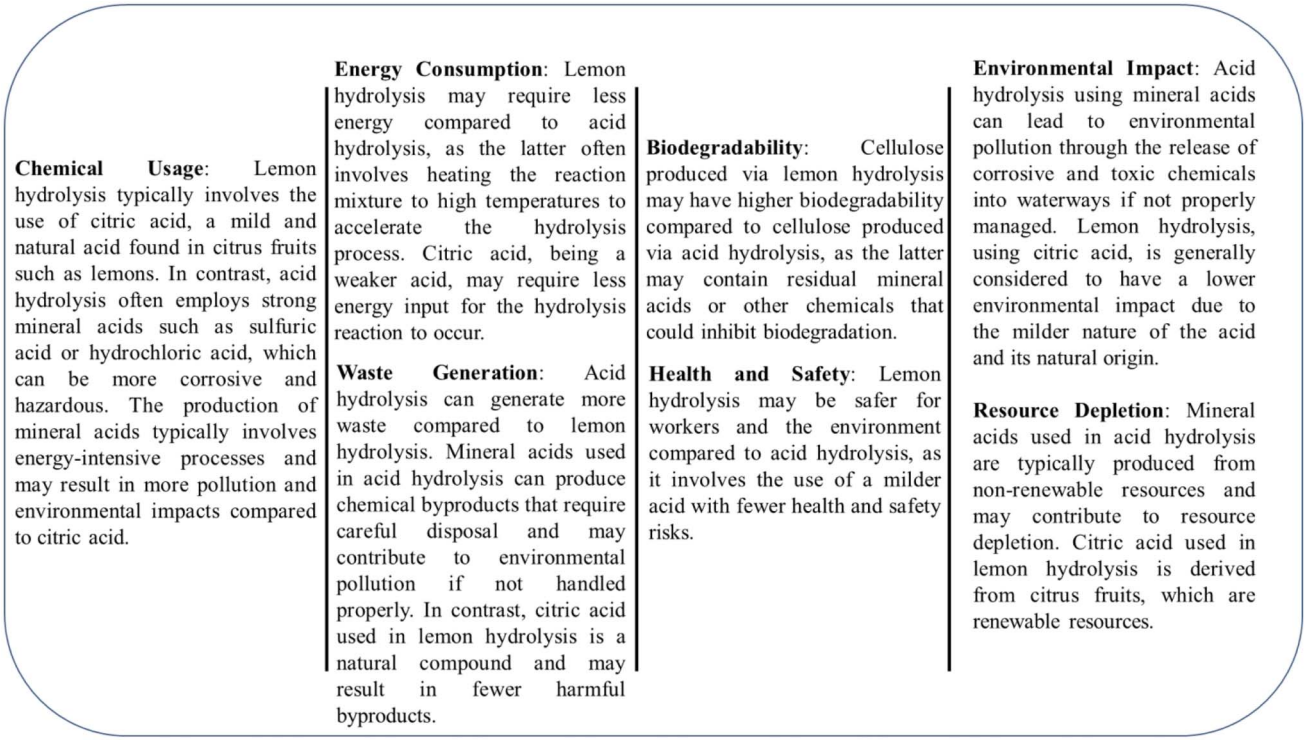

Fig. 9 Sustainability of lemon citric acid hydrolysis *versus* fossil sulphuric acid hydrolysis.

at \$0.10 per liter. It requires the same amount—1 liter—to process 100 grams of coconut husk, resulting in a cost of around \$0.01 per gram of nanocellulose. However, despite its lower price, sulfuric acid introduces significant environmental and safety risks, which increase its overall lifecycle cost.

The energy requirements for both methods are comparable, as both lemon juice and sulfuric acid need sonication and heating for the extraction process. On average, sonication requires 200–300 kJ to process 100 grams of coconut husk, with only minor differences due to the viscosity and acidity of each substance. However, the disposal and safety issues associated with sulfuric acid are more costly. Sulfuric acid requires neutralization and special handling during disposal, leading to additional costs for treatment and waste management. On the other hand, lemon juice, being an organic substance, presents minimal safety hazards and can be disposed of without the need for specialized treatments, thus resulting in lower disposal costs.

From an environmental perspective, sulfuric acid has significant drawbacks. Its hazardous nature necessitates costly waste management procedures to neutralize the acid and dispose of the resulting waste, contributing to its overall environmental impact. Lemon juice, however, is a biodegradable and renewable resource, which means it has a much lower environmental footprint. Using lemon juice instead of sulfuric acid for acid hydrolysis significantly reduces the environmental risks associated with the process and aligns better with sustainability goals.

In terms of overall cost (Table 7), sulfuric acid is slightly cheaper than lemon juice, with the cost per gram of nanocellulose being around \$0.01 for sulfuric acid compared to \$0.015 for lemon juice. However, the additional environmental and safety costs associated with sulfuric acid balance out the price difference, making the total cost difference between the two methods quite narrow. The cost of using lemon juice may be higher in terms of raw materials, but the reduced environmental and safety concerns offset this difference.

Table 7 Comparison of total costs

Cost category	Lemon juice (USD per gram)	Sulfuric acid (USD per gram)
Raw material cost	0.015	0.01
Energy requirements	0.005	0.005
Waste disposal	0.001	0.005
Safety management	0.0005	0.002
Total cost	**0.0215**	**0.022**

In large-scale industrial applications, the cost efficiency of using lemon juice appears more favorable over time. The lower costs associated with safety management and waste disposal make it an attractive alternative. Furthermore, as a renewable resource, lemon juice offers opportunities for sustainable practices. Process optimization, such as increasing the efficiency of lemon juice extraction or using waste lemon juice from the food industry, could further reduce costs. These factors suggest that, while sulfuric acid might have a lower initial raw material cost, lemon juice offers a more sustainable and potentially cost-effective option in the long term.

© 2025 The Author(s). Published by the Royal Society of Chemistry

Open Access Article. Published on 13 May 2025. Downloaded on 2/8/2026 3:31:06 AM. This article is licensed under a Creative Commons Attribution-NonCommercial 3.0 Unported Licence.

End applications of this study

The extraction of cellulose nanofibrils (CNFs) from coconut husk coir using citric acid from lemon juice presents a sustainable way to transform agricultural waste into valuable materials. CNFs have gained significant attention due to their impressive mechanical strength, biodegradability, and versatility. This study not only contributes to waste management but also opens doors for several real-world applications:

• Eco-friendly packaging – with increasing concerns over plastic pollution, CNFs can be used in biodegradable packaging materials, offering an environmentally friendly alternative to synthetic polymers.

• Biomedical and pharmaceutical applications – due to their biocompatibility and non-toxic nature, CNFs have potential uses in wound healing, controlled drug delivery, and even tissue engineering.

• Strengthening bio-composites – CNFs can reinforce natural polymer-based composites, making them stronger and more durable for applications in automotive, aerospace, and construction industries.

• Water purification – CNFs have a high surface area and can be modified to remove contaminants, making them suitable for water filtration systems.

• Food and cosmetics industry – as a natural stabilizer and thickener, CNFs can enhance the texture of food products and cosmetics while ensuring safety and sustainability.

• Energy storage devices – with their unique nanostructure, CNFs are being explored for use in batteries and supercapacitors, potentially improving the efficiency and durability of energy storage solutions.

By utilizing coconut husk coir, which is often discarded as waste, this research supports the idea of a circular economy, where waste materials are upcycled into high-value products. This not only helps reduce environmental pollution but also creates new economic opportunities for industries looking for sustainable alternatives.

Why use lemon juice instead of sulfuric acid?

Traditionally, strong acids like sulfuric acid are used for breaking down cellulose fibers, but they come with major drawbacks. Sulfuric acid-based hydrolysis is aggressive, often leading to excessive cellulose-degradation, while also posing serious environmental and safety concerns due to its corrosive nature and the need for intensive neutralization processes. In this study, citric acid from lemon juice was used as a green alternative, offering several advantages:

– Citric acid is naturally occurring, non-toxic, and breaks down easily in the environment, unlike sulfuric acid, which produces hazardous waste.

– Instead of breaking down cellulose aggressively, citric acid enables a more controlled hydrolysis, retaining the nanofibril structure.

– Unlike strong mineral acids, citric acid is non-corrosive, reducing equipment damage and operational risks in large-scale processing.

– Sulfuric acid hydrolysis requires excessive washing and neutralization, whereas citric acid is milder and requires less water for post-processing.

– Citric acid is already widely used in food, pharmaceutical, and cosmetic industries, meaning its large-scale production is well established. With process optimization, it could be seamlessly integrated into biorefineries focusing on sustainable material extraction.

This study highlights a simple yet effective way to extract nanocellulose without relying on hazardous chemicals. By replacing harmful acids with a natural, biodegradable alternative, this method aligns with the principles of green chemistry and provides a realistic, scalable approach for industrial applications. Given the abundance of coconut husk coir and the growing interest in biodegradable nanomaterials, this research contributes to a more sustainable and eco-conscious future—one where agricultural waste is no longer just discarded, but transformed into something valuable.

Conclusion

The study aimed to explore a green alternative for preparing nanocellulose, replacing harmful mineral acids with organic lemon juice (citric acid) for the hydrolysis of coconut husk coir. SEM analysis confirmed that both the lemon juice citric acid and the mineral sulphuric acid (H_2SO_4) methods efficiently extracted nanocellulose, with visible elongation in the fibrils, indicating effective defibrillation. Dynamic Light Scattering (DLS) and image analysis validated the nanoscale of the fibers, while FTIR analysis indicated successful removal of hemicelluloses and lignin. Notably, the nanocellulose derived from lemon juice exhibited a higher zeta potential of −32 mV and increased interfibrillar repellence, differentiating it from its mineral acid-extracted counterpart. Additionally, the crystallinity of the citric acid-hydrolyzed cellulose surpassed that of the sulphuric acid-hydrolyzed version, at 37%, compared to 32%, as a result of a more restrained acid hydrolysis process, which less disruptively cleaved the glycosidic linkages in cellulose. These findings underscore the viability of the proposed green method in isolating cellulose nanofibrils from coconut coir, offering an environmentally safe alternative to conventional acid hydrolysis.

Data availability

The data generated and analyzed during this study are available from the corresponding author upon reasonable request. Any supplementary information related to the experimental procedures, raw data, or processed results will be provided in compliance with institutional policies and data-sharing guidelines. Where applicable, data will also be made accessible through publicly available repositories, ensuring transparency and promoting further research in the field of sustainable material processing.

Conflicts of interest

The authors have no conflicts of interest to declare.

Open Access Article. Published on 13 May 2025. Downloaded on 2/8/2026 3:31:06 AM. This article is licensed under a Creative Commons Attribution-NonCommercial 3.0 Unported Licence.

Acknowledgements

The authors of this manuscript would like to thank Department of Chemistry, Chandigarh University for their support in the completion of this research work. I also extend my heartfelt thanks to the Instrumentation Laboratory of the Department for granting access to essential analytical facilities and equipment, which were vital for the successful completion of this study.

References

1 P. T. Anastas and E. S. Beach, Green chemistry: The emergence of a transformative framework, *Green Chem. Lett. Rev.*, 2007, **1**(1), 9–24, DOI: **10.1080/17518250701882441**.

2 M. Mutwil, S. Debolt and S. Persson, Cellulose synthesis: a complex complex, *Curr. Opin. Plant Biol.*, 2008, **11**(3), 252–257, DOI: **10.1016/j.pbi.2008.03.007**.

3 J. R. Barnett and V. A. Bonham, Cellulose microfibril angle in the cell wall of wood fibres, *Biol. Rev. Cambridge Philos. Soc.*, 2004, **79**(2), 461–472, DOI: **10.1017/S1464793103006377**.

4 Y. Nishiyama, Structure and properties of the cellulose microfibril, *J. Wood Sci.*, 2009, **55**(4), 241–249, DOI: **10.1007/s10086-009-1029-1**.

5 J. M. Dugan, J. E. Gough and S. J. Eichhorn, Bacterial cellulose scaffolds and cellulose nanocrystals for tissue engineering, *Nanomedicine*, 2013, **8**(2), 287–298, DOI: **10.2217/nnm.12.211**.

6 A. Blanco, M. C. Monte, C. Campano, A. Balea, N. Merayo and C. Negro, *Nanocellulose for Industrial Use: Cellulose Nanofibrils (CNF), Cellulose Nanocrystals (CNC), and Bacterial Cellulose (BC)*, Elsevier Inc., 2018, DOI: **10.1016/B978-0-12-813351-4.00005-5**.

7 R. Meesupthong, N. Yingkamhaeng, T. Nimchua, P. Pinmanee, S. I. Mussatto and P. Sukyai, Xylanase pretreatment of energy cane enables facile cellulose nanocrystal isolation, *Cellulose*, 2021, **28**, 799–812.

8 T. C. Mokhena and M. J. John, Cellulose nanomaterials: New generation materials for solving global issues, *Cellulose*, 2020, **27**, 1149–1194.

9 E. Abraham, B. Deepa, L. A. Pothan, M. Jacob, S. Thomas, U. Cvelbar, *et al.*, Environmental friendly method for the extraction of coir fibre and isolation of nanofibre, *Carbohydr. Polym.*, 2013, **92**(2), 1477–1483, DOI: **10.1016/j.carbpol.2012.10.056**.

10 B. Aaliya, K. V. Sunooj and M. Lackner, Biopolymer composites: a review, *Int. J. Biobased Plast.*, 2021, **3**(1), 40–84, DOI: **10.1080/24759651.2021.1881214**.

11 A. S. Azmi, N. Atiqah, B. Ahmad, P. Me, A. Ismail and N. Ngadiman, *Study on Mechanical Properties of Organic and Non-Organic Fibre Panel Board*, 2022, vol. 3, 1, pp. 266–281.

12 D. Trache, M. H. Hussin, M. K. M. Haafiz, V. K. Thakur, A. Alfattah, E. B. Yahya, *et al.*, Recent progress in cellulose nanocrystals: sources and production, *Nanoscale Res. Lett.*, 2017, **9**(5), 1763–1786, DOI: **10.1039/C6NR09494E**.

13 J. Wu, X. Du, Z. Yin, S. Xu, S. Xu and Y. Zhang, Preparation and characterization of cellulose nanofibrils from coconut coir fibers and their reinforcements in biodegradable composite films, *Carbohydr. Polym.*, 2019, **211**, 49–56, DOI: **10.1016/j.carbpol.2019.01.093**.

14 W. Stelte, T. Nørgaard, A. R. Sanadi, J. Ahrenfeldt, T. Thomsen and U. B. Henriksen, Coir from coconut processing waste as a raw material for applications beyond traditional uses, *BioResources*, 2023, **18**(1), 2187–2212.

15 L. Ravindran, M. S. Sreekala and S. Thomas, Novel processing parameters for the extraction of cellulose nanofibres (CNF) from environmentally benign pineapple leaf fibres (PALF): Structure-property relationships, *Int. J. Biol. Macromol.*, 2019, **131**, 858–870, DOI: **10.1016/j.ijbiomac.2019.03.134**.

16 R. Kumar, B. Rai, S. Gahlyan and G. Kumar, A comprehensive review on production, surface modification and characterization of nanocellulose derived from biomass and its commercial applications, *eXPRESS Polym. Lett.*, 2021, **15**(2), 104–120, DOI: **10.3144/expresspolymlett.2021.11**.

17 H. Ji, Z. Xiang, H. Qi, T. Han, A. Pranovich and T. Song, Strategy towards one-step preparation of carboxylic cellulose nanocrystals and nanofibrils with high yield, carboxylation and highly stable dispersibility using innocuous citric acid, *Green Chem.*, 2019, **21**(8), 1956–1964.

18 F. Fahma, S. Iwamoto, N. Hori, T. Iwata and A. Takemura, Effect of pre-acid-hydrolysis treatment on morphology and properties of cellulose nanocrystals from coconut husk, *Cellulose*, 2011, **18**(2), 443–450, DOI: **10.1007/s10570-010-9480-0**.

19 S. Ventura-Cruz and A. Tecante, Extraction and characterization of cellulose nanofibrils from Rose stems (Rosa spp.), *Carbohydr. Polym.*, 2019, **220**, 53–59, DOI: **10.1016/j.carbpol.2019.05.053**.

20 A. Alemdar and M. Sain, Biocomposites from wheat straw nanofibrils: Morphology, thermal and mechanical properties, *Compos. Sci. Technol.*, 2008, **68**(2), 557–565, DOI: **10.1016/j.compscitech.2007.05.044**.

21 A. K. Trivedi and M. K. Gupta, An efficient approach to extract nanocrystalline cellulose from sisal fibers: Structural, morphological, thermal and antibacterial analysis, *Int. J. Biol. Macromol.*, 2023, **233**, 123496, DOI: **10.1016/j.ijbiomac.2023.123496**.

22 Y. Mao, K. Liu, C. Zhan, L. Geng, B. Chu and B. S. Hsiao, Characterization of nanocellulose using small-angle neutron, X-ray, and dynamic light scattering techniques, *J. Phys. Chem. B*, 2017, **121**(6), 1340–1351, DOI: **10.1021/acs.jpcb.6b11425**.

23 C. S. Julie Chandra, N. George and S. K. Narayanankutty, Isolation and characterization of cellulose nanofibrils from arecanut husk fibre, *Carbohydr. Polym.*, 2016, **142**, 158–166, DOI: **10.1016/j.carbpol.2016.01.015**.

24 Y. Nishiyama, P. Langan and H. Chanzy, Crystal structure and hydrogen-bonding system in cellulose Iβ from synchrotron X-ray and neutron fiber diffraction, *J. Am. Chem. Soc.*, 2002, **124**(31), 9074–9082.

25 S. Park, J. O. Baker, M. E. Himmel, P. A. Parilla and D. K. Johnson, Cellulose crystallinity index: measurement

 © 2025 The Author(s). Published by the Royal Society of Chemistry

Open Access Article. Published on 13 May 2025. Downloaded on 2/8/2026 3:31:06 AM. This article is licensed under a Creative Commons Attribution-NonCommercial 3.0 Unported Licence.

techniques and their impact on interpreting cellulase performance, *Biotechnol. Biofuels*, 2010, **3**, 10.

26 Y. Mao, K. Liu, C. Zhan, L. Geng, B. Chu and B. S. Hsiao, Characterization of nanocellulose using small-angle neutron, X-ray, and dynamic light scattering techniques, *J. Phys. Chem. B*, 2017, **121**(6), 1340–1351, DOI: **10.1021/acs.jpcb.6b11425**.

27 X. Yang, *et al.*, Effects of preparation methods on the morphology and properties of nanocellulose (NC) extracted from corn husk, *Ind. Crops Prod.*, 2017, **109**, 241–247, DOI: **10.1016/j.indcrop.2017.08.032**.

28 A. K. Krishnan, C. Jose, K. R. Rohith and K. E. George, Sisal nanofibril reinforced polypropylene/polystyrene blends: Morphology, mechanical, dynamic mechanical and water transmission studies, *Ind. Crops Prod.*, 2015, **71**, 173–184, DOI: **10.1016/j.indcrop.2015.03.076**.

29 S. Beck, M. Méthot and J. Bouchard, General procedure for determining cellulose nanocrystal sulfate half-ester content by conductometric titration, *Cellulose*, 2015, **22**, 101–116.

30 H. Kalita, A. Hazarika, R. Kandimalla, S. Kalita and R. Devi, Development of banana (Musa balbisiana) pseudo stem fiber as a surgical bio-tool to avert post-operative wound infections, *RSC Adv.*, 2018, **8**(64), 36791–36801, DOI: **10.1039/C8RA04470H**.

31 B. M. Cherian, A. L. Leão, S. F. de Souza, S. Thomas, L. A. Pothan and M. Kottaisamy, Isolation of nanocellulose from pineapple leaf fibres by steam explosion, *Carbohydr. Polym.*, 2010, **81**(3), 720–725, DOI: **10.1016/j.carbpol.2010.03.046**.

32 F. C. Claro, C. Jordão, B. M. de Viveiros, L. J. E. Isaka, J. A. Villanova Junior and W. L. E. Magalhães, Low cost membrane of wood nanocellulose obtained by mechanical defibrillation for potential applications as wound dressing, *Cellulose*, 2020, **27**(18), 10765–10779, DOI: **10.1007/s10570-020-03129-2**.

33 D. Pawcenis, M. Leśniak, M. Szumera, M. Sitarz and J. Profic-Paczkowska, Effect of hydrolysis time, pH and surfactant type on stability of hydrochloric acid hydrolyzed nanocellulose, *Int. J. Biol. Macromol.*, 2022, **222**, 1996–2005.

34 S. P. Bangar, M. M. Harussani, R. A. Ilyas, A. O. Ashogbon, A. Singh, M. Trif and S. M. Jafari, Surface modifications of cellulose nanocrystals: Processes, properties, and applications, *Food Hydrocolloids*, 2022, **130**, 107689.

35 F. T. Seta, X. An, L. Liu, H. Zhang, J. Yang, W. Zhang, *et al.*, Preparation and characterization of high yield cellulose nanocrystals (CNC) derived from ball mill pretreatment and maleic acid hydrolysis, *Carbohydr. Polym.*, 2020, **234**, 115942.

36 A. Gaikwad, Effect of particle size on the kinetics of enzymatic hydrolysis of microcrystalline cotton cellulose: a modeling and simulation study, *Appl. Biochem. Biotechnol.*, 2019, **187**(3), 800–816.

37 T. Heinze, Cellulose: structure and properties, in *Cellulose Chemistry and Properties: Fibers, Nanocelluloses and Advanced Materials*, 2016, pp. 1–52.

38 K. B. Mir and N. A. Khan, Solid dispersion: Overview of the technology, *Int. J. Pharma Sci. Res.*, 2017, **8**(6), 2378–2387.

39 K. Vilkhu, R. Mawson, L. Simons and D. Bates, Applications and opportunities for ultrasound assisted extraction in the food industry—A review, *Innovative Food Sci. Emerging Technol.*, 2008, **9**(2), 161–169.

© 2025 The Author(s). Published by the Royal Society of Chemistry